

Relaxation of the excess magnetization of random-field-induced metastable domains in $\text{Fe}_{0.47}\text{Zn}_{0.53}\text{F}_2$

S-J. Han and D. P. Belanger

Physics Department, University of California–Santa Cruz, Santa Cruz, California 95064

W. Kleemann

Angewandte Physik, Universität Duisburg, 4100 Duisburg, Germany

U. Nowak

Theoretische Tieftemperaturphysik, Universität Duisburg, 4100 Duisburg, Germany

(Received 30 August 1991)

The Faraday rotation of the excess magnetization in the field-cooled random-field Ising antiferromagnet $\text{Fe}_{0.47}\text{Zn}_{0.53}\text{F}_2$ has been measured for fields $0 < H < 7$ T applied along the easy axis at temperatures $5 \text{ K} < T < 22 \text{ K}$, well below the $H=0$ phase transition occurring at $T = T_N (= 37 \text{ K})$. The relaxation of the excess magnetization, which is proportional to the Faraday rotation, does not follow the Nattermann-Vilfan theory in detail for this range of T and H . We explore other possible forms for the time dependence of the excess magnetization and use Monte Carlo techniques as an aid in the interpretation of the experimental data.

I. INTRODUCTION

Considerable attention has been directed to the dynamics of magnetic systems with quenched randomness.^{1–6} Among the ideal random systems in which to study dynamics is the dilute Ising antiferromagnet, of which $\text{Fe}_x\text{Zn}_{1-x}\text{F}_2$ is one of the best examples for three dimensions ($d=3$). The static and dynamic critical behaviors have been studied for $H=0$ and magnetic concentrations $0.31 < x < 1$, which corresponds to the random-exchange Ising model (REIM). Well above the percolation threshold ($x_p=0.24$ for $\text{Fe}_x\text{Zn}_{1-x}\text{F}_2$), the REIM dynamics near the transition temperature T_N appear similar to that of the pure FeF_2 system, but with a much longer characteristic time for relaxation. For example, the relaxation rate of $\text{Fe}_{0.46}\text{Zn}_{0.54}\text{F}_2$ has been shown⁷ to be 2 orders of magnitude smaller than that of pure FeF_2 .

The random-field Ising model (RFIM), created in dilute antiferromagnets⁸ when a field $H > 0$ is applied collinear with the spin ordering axis, is strikingly different from the REIM. The static critical behaviors of the $d=2$ and 3 REIM and RFIM belong to very distinct universality classes. Moreover, random fields fundamentally change the character of the relaxation towards the ground state. Relaxation rates of hours or longer can be readily observed near the phase transition in specific heat, neutron scattering, and many other experiments. An important consequence of the extreme critical slowing down in the $d=3$ RFIM is that a sample cooled in the presence of a magnetic field never achieves long-range order^{9,10} below $T_c(H)$. Instead, a metastable domain structure forms. To study RFIM critical behavior, one must first cool the sample in zero field, achieving long-range order via the REIM transition, subsequently turn the field on, and then heat the system. One can then observe dynam-

cally rounded critical behavior near $T_c(H)$. The RFIM dynamic critical behavior has been characterized using ac susceptibility techniques and appears to be best described in terms of activated dynamics.^{11,12} One result of the extreme critical slowing near the transition is that experiments which normally are considered to measure the static properties, specific-heat experiments for example, must be interpreted with dynamical effects taken into consideration. Close to $T_c(H)$, but outside the dynamically rounded region, a crossover from REIM to new RFIM critical behavior for the specific heat,^{13,14} correlation length,⁹ and staggered susceptibility⁹ is observed.

Extremely slow time-dependent behavior dominates well below $T_c(H)$ as well. The metastable domain state, induced by cooling the crystal in a field (FC), shows essentially no observable time dependence well below T_c in neutron scattering or Faraday rotation experiments provided the field is held constant.^{9,10,15} Although very minor relaxation effects have been observed in $\text{Fe}_{0.46}\text{Zn}_{0.54}\text{F}_2$ at high fields and at temperatures close to the phase boundary $T_c(H)$ by using SQUID techniques,¹⁶ the system essentially does not relax toward its ground state at lower temperatures, $T < 0.5T_c(H)$, on easily observable time scales as long as the pinning effects of the random field remain. On the other hand, after cooling to low T , one can rapidly reduce the field to zero, removing the random-field pinning and allowing the system to evolve in time via low-temperature REIM dynamics. Significant pinning now originates from the magnetic vacancies and is possibly influenced by dipolar interactions¹⁷ between different metastable domains. It has been shown with neutron scattering that even after the external field is removed, the length scale associated with the metastable domain structure does not vary significantly with time at low enough T . Faraday rotation measure-

ments indicate that the excess magnetization can be largely recovered after the sample has been evolving at $H=0$ by reapplying the uniform field. These observations, that the domain size does not evolve with time and that the excess magnetization is recoverable by reapplication of the field, indicate that the decay of the excess magnetization comes only from largely reversible rearrangements of domain walls on a local scale of a few lattice spacings and not from macroscopic changes in domain structure, which would be irreversible. Domain walls reside largely on the vacancies and are quite effectively pinned on large scales. Nattermann and Vilfan¹⁸ (NV) have developed a scaling theory for the time dependence of the excess magnetization based on the idea that the domain walls rearrange with time only on a local scale but the characteristic domain size does not vary with time. Wherever a domain wall occurs in the presence of the applied field, the spins immediately to either side of the wall are predominantly aligned collinearly with the field, creating the excess magnetization. A small contribution to the excess magnetization originates from the statistical imbalance of the number of spins in a given domain, which determined the initial orientation of the domain while it formed upon cooling of the crystal in the field. If the domain walls are stable at low T on macroscopic length scales, the volume term will be essentially constant. The NV model, which is expected to be valid at low T , yields a time dependence from domain-wall readjustment

$$M_r(t) = A \ln^{-\psi}(t/t_0) + B, \quad (1)$$

where $\psi \approx 0.4$, t_0 is the microscopic time of the order of 10^{-12} sec, and B is the small constant term originating from the volume effect. The Faraday rotation technique is a convenient and sensitive probe of the excess uniform magnetization originating from the domain structure.¹⁹ Early measurements on the Ising antiferromagnets $\text{Fe}_{0.47}\text{Zn}_{0.53}\text{F}_2$ and $\text{Fe}_{0.7}\text{Mg}_{0.3}\text{Cl}_2$ indicate reasonable agreement with the theory by setting $\psi=1$ and $B=0$ if t_0 is replaced by a parameter τ which decreases exponentially with temperature.^{15,20} Later on, Eq. (1) was tested more rigorously on $\text{Fe}_{0.7}\text{Mg}_{0.3}\text{Cl}_2$.²¹ Systematic variations of both ψ and B were found upon varying H and/or T . Only in the low- H and low- T limit was the NV prediction found to hold approximately. However, systematic departures from the NV equation are discernible. Clearly, further efforts were needed to more precisely test the theory. We report results of experiments that measure, with improved precision, the time dependence of the Faraday rotation. We also present data obtained from Monte Carlo simulations which make clear the importance of the finite time taken in the experiments to turn off the large magnetic fields and aid in the interpretation of the experimental data. Using these data and the simulations, we find two empirical equations that fit the experimental data better than the NV equation. One is a power law in t used previously to analyze Monte Carlo simulations^{22,23} and the other is a generalization of the power law. We discuss fits of experimental data to all three expressions.

II. EXPERIMENTAL DETAILS

The single crystal of $\text{Fe}_{0.47}\text{Zn}_{0.53}\text{F}_2$ is the same one used in previous Faraday rotation studies.^{15,19} The concentration has been determined to vary less than $\delta x = 5 \times 10^{-4}$ along the beam path. The optical arrangement used in these measurements has also been described previously.²⁴ By removing depolarized stray light with a pin hole of 0.3 mm diameter behind the sample, we were able to increase the rotation-angle resolution in the present experiments. The data were obtained using a cryostat with a split coil arrangement allowing fields up to $H=7$ T to be applied along the c axis of the crystal. The sample temperature was measured with a carbon thermometer and maintained using a cold finger. One difficulty encountered in the experiment is that a significant time, e.g, 170 sec for $H=5$ T, was required to reduce the field to zero. This time, t_w , is necessary to avoid generating eddy current heating in the sample holder at a rate too large for the temperature controller to compensate. As we will discuss, the time t_w is found always to be a significant consideration when analyzing the data. Computer simulations prove to be very useful in this regard.

III. EXPERIMENTAL RESULTS

For each run, the crystal was rapidly cooled, over a period of a few minutes, in the presence of a field H from well above the phase boundary $T_c(H)$ to a temperature $T < T_c(H)$ to achieve a quenched random-field-induced metastable domain state. At low temperatures, $T < 0.5T_N$ [$T_N = T_c(H=0)$], no time dependence was observed for $H \leq 5$ T (see also Ref. 16). However, we have seen a very small time dependence in the signal at $T=5$ and 6.5 K with $H=6$ and 7 T. The initial decrease in the remanent magnetization [$M_r(t)$], occurring while H is de-

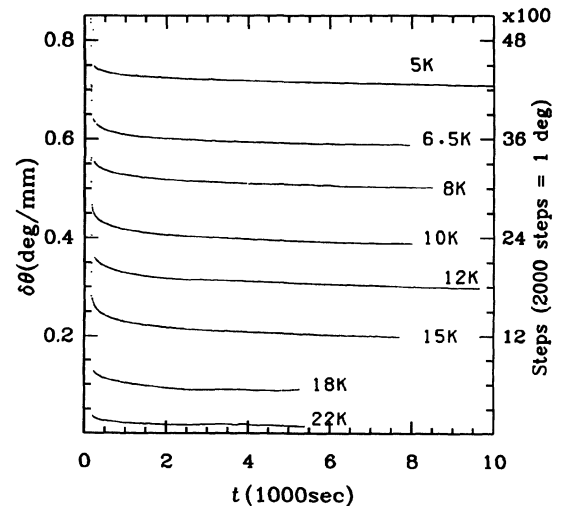


FIG. 1. $\delta\theta(t)$, which is proportional to $M_r(t)$, vs t for $H=5$ T at several different temperatures, $T=5, 6.5, 8, 10, 12, 15, 18,$ and 22 K. The left scale shows $\delta\theta(t)$ in units of degrees per mm and the right scale is in digitized steps, where one step is about the experimental angular resolution.

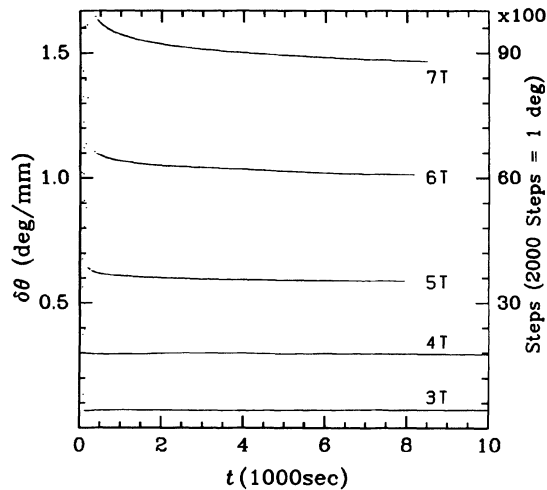


FIG. 2. $\delta\theta(t)$ vs t at $T=6.5$ K for several different fields, $H=3, 4, 5, 6,$ and 7 T.

creasing, is extremely large and rapid relative to the subsequent $H=0$ time dependence. We show $M_r(t)$ vs t for $H=5$ T at several different temperatures, $T=5, 6.5, 8, 10, 12, 15, 18,$ and 22 K in Fig. 1. As expected, the magnitude of the remanent magnetization, remaining after the sample is prepared via FC and the field H is subsequently removed, decreases as thermal fluctuations become more important with increasing T . Figure 2 shows $M_r(t)$ vs t for $T=6.5$ K at several fields, $H=3, 4, 5, 6,$ and 7 T. The remanent magnetization increases with the strength of the effective random field which is proportional to H .²⁵ The remanent magnetization after the field H is removed is only observable for temperatures well below T_N . In Figs. 1 and 2, the zero of time ($t=0$) is taken to be the moment the field begins to decrease. Figure 3 shows the logarithm of the remanent magnetization for

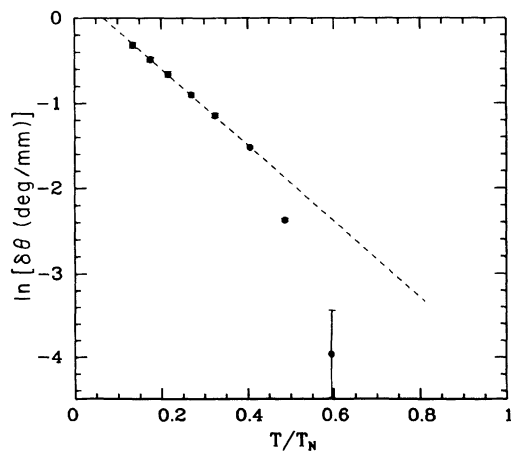


FIG. 3. $\ln(\delta\theta)$ vs T/T_N at an arbitrarily chosen time $t=2000$ sec. The data were taken after FC and reducing the field from $H=5$ T to zero at $T=5, 6.5, 8, 10, 12, 15, 18,$ and 22 K. The dashed line indicates the approximate logarithmic behavior for $T < 15$ K. Above $0.5T_N$ more rapid decay is apparent.

$H=5$ T at an arbitrarily chosen time $t=2000$ sec vs T/T_N . For $T \lesssim 15$ K ($0.41T_N$), $\ln(\delta\theta)$ is nearly proportional to $-T$. For greater T , the remanent magnetization falls off much more rapidly. We found the remanent signal to be essentially unobservable for $T > 22$ K ($0.6T_N$).

IV. ANALYSIS AND DISCUSSION

The large, rapid initial decrease in the remanent magnetization, which we have observed while H was decreasing rapidly, originates predominantly from isolated spins and single bond spins aligned with the direction of the external magnetic field which has a strength comparable to that of the single bond exchange field (~ 7 T).²⁶ Some portion is also coming from fully frustrated single spins, e.g., a spin with two neighbor spins whose directions are opposite to each other and are relatively stable over times used to turn the external field on and off. Such frustrated spins behave in a manner very similar to the isolated spins. We base these comments on the behavior observed directly in computer simulations.²⁷

We have tried several equations for the data analysis and will discuss three of them in detail below. We will use one specific data set, at $H=7$ T and $T=6.5$ K, for comparing the fits to the different functions. The results are typical of all the data sets. Before discussing these functions, we need to comment in more detail on the waiting time t_w and how it may be dealt with in the data analysis. Since the typical waiting time is very small compared with the total time of a run, it might have been assumed that it is of no significance in the interpretation of the data. However, although a typical waiting time in our experiment is less than 2.5% of the total run time, we can demonstrate that it is still not negligible. Since t_w is finite, the zero of the time for fitting to an appropriate decay law could be effectively at some moment between 0 and t_w . Hence, we set $t \rightarrow t - \alpha t_w$ with the free parameter $0 < \alpha < 1$. In Fig. 4, we show $\ln(\delta\theta)$ vs $\ln(t)$ for two extreme choices, $\alpha=0$ and 1, using data at $T=15$ K and

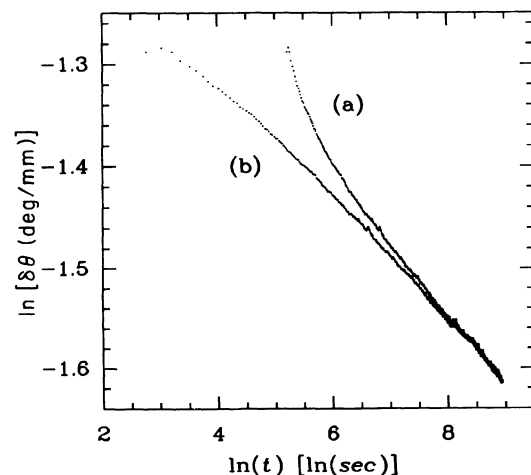


FIG. 4. $\ln(\delta\theta)$ vs $\ln(t)$ for $H=5$ T at $T=15$ K with two extreme α settings (see text). The concave shape, curve (a), is with $\alpha=0$. The convex shape, curve (b), is with $\alpha=1$.

$H=5$ T, where $t_w=169$ sec. Curve (a) in this figure is for $\alpha=0$, which corresponds to the slow decay of the magnetization starting as soon as the external field begins to decrease. Curve (b) is for $\alpha=1$, which would be the case if the relaxation from random-exchange interactions begins at the moment the external magnetic field becomes zero. Obviously the description of the nature of the decay curves depends crucially on the choice of α . In order to gain insight into this problem, we used computer simulations with a $61 \times 61 \times 60$ cubic lattice with 50% of the sites randomly occupied magnetic sites and with nearest-neighbor Ising antiferromagnetic interactions, J , and periodic boundary conditions. The system was prepared with a random spin configuration, i.e., a very high-temperature state. Quenching to a temperature $T=0.4$ J ($\approx 0.2T_N$), a magnetic field $H=1.5$ J was applied for 1000 Monte Carlo steps (MCS), i.e., an average of 1000 spin flips per spin. Subsequently, the magnetic field was turned off in one of two ways. The first case, shown in Fig. 5, curve (a), is for the field being turned off instantly, i.e., $t_w \approx 0$. In the second case, shown in Fig. 5, curve (b), the field was slowly turned off through another 1000 MCS, with the field strength decreasing linearly with the number of MCS, i.e., $t_w=1000$ MCS. In analyzing this stimulation data, we use the power law

$$M_r(t) = M_0 t^{-\alpha}, \quad (2)$$

to be discussed more fully below, as a trial function. For the first case, α must be essentially zero. For the second case, analysis of the computer-simulation data gives an effective $\alpha \approx 0.9$ when we require the fit of the data to yield results comparable to the first case. Detailed parameters for these comparisons are given in Table I. These examples are typical and we always find α much closer to unity than to zero. Longer times do not appreciably affect these results for α . For this range of t there is little effect from increasing L , though some finite-size effects can be observed at much longer times. However,

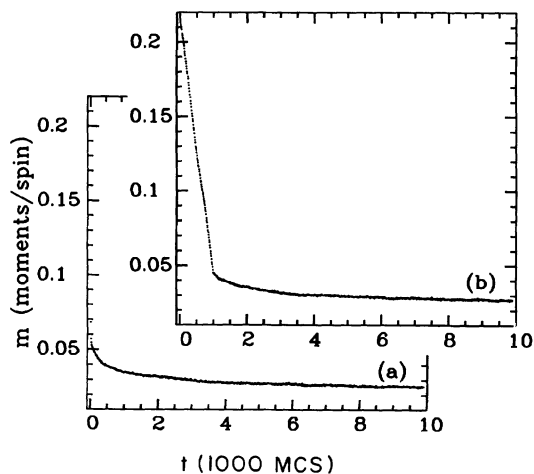


FIG. 5. Monte Carlo data M_r vs t for $H=1.5$ J at $T=0.4$ J. Curve (a) shows the remanent magnetization after turning off the field instantly. For curve (b) the field is turned off linearly during the first 1000 MCS. The curves are offset for clarity.

increasing L does not appreciably affect the value obtained for α .

An analysis of the $\delta\theta$ vs t data was first attempted using the NV function [Eq. (1)]. Figure 6 shows a typical fit, when we set the zero of time to be the moment the field starts to decrease ($\alpha=0$), to the $\delta\theta$ vs t data taken at $T=6.5$ K for the system prepared via FC with $H=7$ T. The parameters for this fit are $A=105.2 \pm 0.36$ deg/mm, $\psi=1.1864 \pm 0.00097$, $t_0=10^{-12}$ sec, and $B=0$ (fixed). In this case, the fit quality is fair, but there are apparent systematic deviations. If, instead, we allow α to be a free parameter, a much better fit is found with $\alpha \approx 0.68$ which is somewhat smaller than the value obtained from the simulation described above. Since the parameter α plays a crucial role in fitting the initial curvature, the fit shows a much better fit for the first 10^3 sec of data when α is allowed to vary. Nevertheless, the data and fit start to deviate at longer times, more so than with $\alpha=0$. Figure 7 shows the deviations of the data from the fit when α is allowed to be a free parameter. In this fit $\alpha=0.68$, $A=74.86 \pm 0.057$ deg/mm, $\psi=1.0918 \pm 0.00021$, $t_0=10^{-12}$ sec (fixed), and $B=0$ (fixed). Although some parameter values have changed, we find that the behavior of the parameters, particularly ψ , is not significantly different from the fit with α fixed to zero. Since allowing the parameter α to vary improves the fit only for small t , a more sophisticated model assuming some distribution of starting times for the random processes involved in the domain evolution cannot reduce the deviations of the data from the NV fit at longer times. To illustrate the temperature dependence of the behavior of the exponent ψ , we show in Fig. 8(a) ψ vs T obtained from fits to Eq. (1) with B fixed to zero and for the three cases $t_0=10^{-9}$, 10^{-12} , and 10^{-15} sec representing a reasonable range of microscopic times. In all cases the exponent increases rapidly with T in agreement with previous results on $\text{Fe}_{0.7}\text{Mg}_{0.3}\text{Cl}_2$.²¹ To investigate the influence of the B

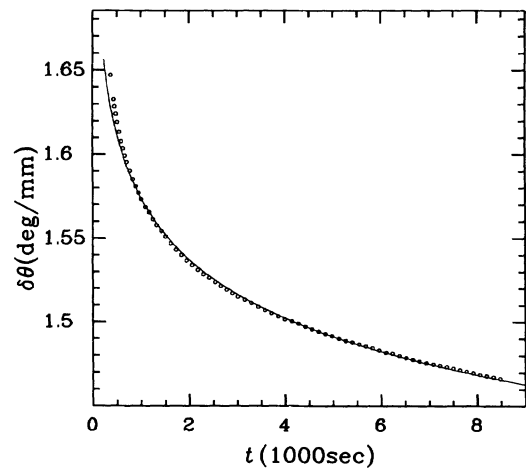


FIG. 6. $\delta\theta$ vs t and a fit to the NV function, with $\alpha=0$ at $T=6.5$ K for $H=7$ T. For clarity, less than 10% of the actual data are shown in this figure. Some systematic deviation of the data from the fit is seen in this fit which yields the exponent $\psi=1.186$.

TABLE I. Fit parameters referring to Fig. 5 (see text).

t_w	$M_r(t)$	M_0	x	α	χ^2
1	$M_0(t - \alpha t_w)^{-x}$	0.093 3	0.141 0	0.000 01	2.2×10^{-4}
1000	$M_0 t^{-x}$	0.156 0	0.194 4		7.1×10^{-4}
	$M_0(t - \alpha t_w)^{-x}$	0.086 6	0.129 2	0.876 3	1.8×10^{-4}

term in Eq. (1), we fixed $t_0 = 10^{-12}$ sec and fit the data for the four cases $B = 0, 0.017, 0.05,$ and 0.083 deg/mm as shown in Fig. 8(b). Again, ψ increases rapidly with T . We can conclude that the large increase of ψ with T is not strongly sensitive to the values of B and t_0 . The new parameter α does not significantly alter this behavior, even if the fit itself is improved by it. Furthermore, the exponent is only close to the predicted NV value $\psi = 0.4$ for the lowest T investigated. It is not known yet whether the NV theory will hold for $T < 5$ K, or whether the exponent will continue to decrease towards zero. The temperature and field dependence of the exponent observed in fits of the experimental data to the NV equation are qualitatively similar to what has been seen in other experiments^{15,20,21} and computer simulations.²² If we force the exponent to be fixed at the predicted value $\psi = 0.4$, the fit to the data yields unphysical values for t_0 and/or B , e.g., large negative values of B , in Eq. (1) or t_0 many orders of magnitude outside the range given above. It is clear that the data are not adequately described by the NV theory in the temperature and field range investigated. This may indicate that the data were obtained for temperatures too high for the Nattermann-Vilfan theory to hold or may result from an inadequacy of the NV theory.

One of the assumptions of the NV theory is that, at every time t , there is a typical length scale $L(t)$ in the system, which is predominantly responsible for the relaxation at this time. This assumption may be in contradiction to the recent finding that the domains of the FC state are fractals,²⁸ i.e., that there is no typical length scale in the system. A lack of typical length scales in a dynamic

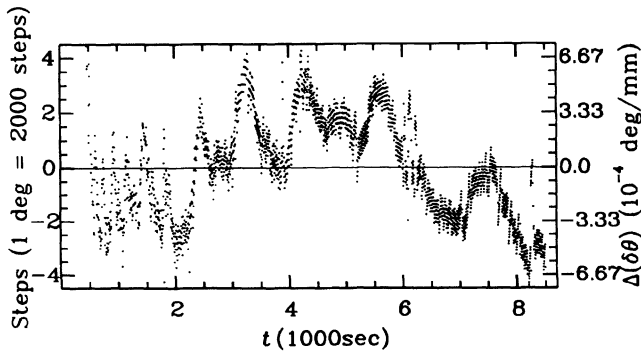


FIG. 7. The deviation of the fit to the NV function from the data with the best fit values $\alpha = 0.68$, $A = 74.86$ deg/mm, $\psi = 1.092$, $t_0 = 10^{-12}$ sec, and $B = 0$. In this case we have shown all of the data, in contrast to the previous figure. Although the fit itself is greatly improved over the case $\alpha = 0$, the systematic deviation of the data from the fit is still clear.

system can be thought to result in a lack of typical time scales, thus yielding a temporal power law.²³

The power law in Eq. (2) has been used to analyze data obtained from Monte Carlo simulations of a diluted anti-ferromagnetic Ising model on a simple-cubic lattice by Nowak and Usadel²³ and was found to be quite adequate. We therefore employed this function to analyze our experimental data and found behavior, particularly with regard to the exponent x , resembling the previous simulation data analyses. The simulations and experiments seem to yield consistent behavior. An example of a fit of the experimental data to Eq. (2) is shown in Fig. 9, where the parameters $M_0 = 1.9263 \pm 0.0001$ deg/mm and $x = 0.03021 \pm 0.00001$ describe the data at $T = 6.5$ K, $H = 7$ T very well. In this analysis, we obtain $\alpha \approx 0.84$, consistent with the value suggested by the simulation result described above. The computer fitting shows extremely small error estimates for each parameter as long as the constant volume term B is kept small (zero in the fit shown in Fig. 9). The B term will be discussed further later. Most data sets yield noticeably better fits to this power law than with the NV function, just as the previous results indicated for the Monte Carlo simulation data. Taking into account the nonuniversal behavior of the exponent x , this function describes the experimental data very well.

In further analyzing the experimental data with various empirical forms for the decay of the remanent mag-

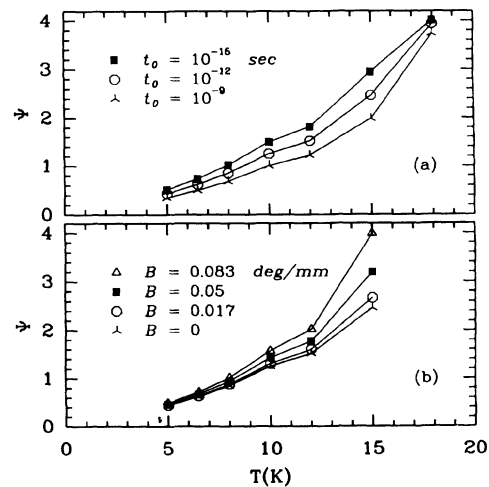


FIG. 8. ψ vs T for $H = 5$ T from fits to the NV function [Eq. (1)] with different values of t_0 and B . (a) shows the temperature-dependent behavior of ψ with $B = 0$ for $t_0 = 10^{-9}, 10^{-12},$ and 10^{-15} sec. (b) is for $t_0 = 10^{-12}$ sec and $B = 0, 0.017, 0.05,$ and 0.083 deg/mm.

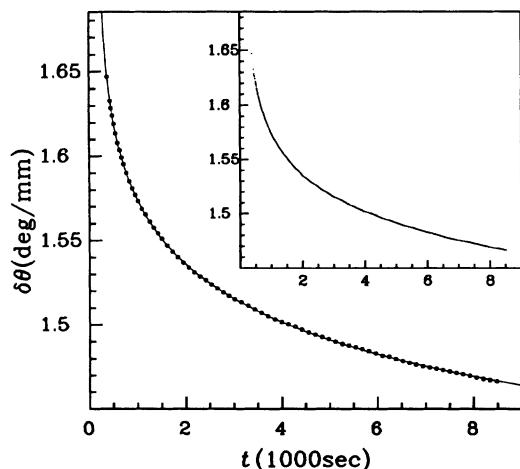


FIG. 9. $\delta\theta$ vs t for $H=7$ T at $T=6.5$ K and a best fit to the power law in Eq. (2). For clarity, less than 10% of the data are shown in the lower curve. The curve represents the best fit with $M_0=1.9263$ deg/mm and $x=0.03$. The fit yields $\alpha=0.84$ and about 32% reduction in χ^2 from a best fit with the NV function in Eq. (1). The systematic deviations are very small, as can be seen by the fact that the fit passes near the center of most circles representing the data. All of the data are shown in the upper curve to illustrate the nature of the fluctuations in the data. A fit to the more general form in Eq. (3) is indistinguishable by eye from the fit shown and yields $M_0=1.870$ deg/mm, $A=0.02$, $y=1.13$, and $\alpha=0.94$. χ^2 is 11% smaller than that obtained with the power law, indicating a better fit.

netization, we found a generalization of the power law in the form

$$M_r(t) = M_0 \exp\{-A[\ln(t/t')]^y\}, \quad (3)$$

which describes the data remarkably well. An attractive feature of fits of the data to this function is that the measured parameters are well behaved with respect to T and H in the sense that the parameter M_0 is consistent with the experimental data, i.e., the value of the function at $t=t'$ as an initial point is less than the in-field value and appears consistent with an extrapolation of the zero-field data to $t=t'$. Most importantly, the exponent y appears as a constant, showing only very small fluctuations between runs at different T and H . The power law in Eq. (2) is a special case of this more general function, with $y=1$. The generalized function in Eq. (3) exhibits faster relaxation at large t than does the power law if $y > 1$, and slower relaxation if $y < 1$. Using the general form, we have found from fits to the experimental data that y is always slightly greater than unity and exhibits very little T and H dependence. Visually, a fit of the data to Eq. (3) is indistinguishable from the fit shown in Fig. 9. Such a fit, with the parameters $M_0=1.870 \pm 0.0029$ deg/mm, $A=0.0203 \pm 0.00048$, $y=1.128 \pm 0.0078$, $\alpha=0.94$ and $t'=1$ sec, is better than can be obtained using the power law shown in Fig. 9. In judging the goodness of the fits for the power law and more general form, we can use not only the χ^2 test but also examine the systematic deviations of the data from the fits, as described for the NV fit

above. We fit the data to Eqs. (2) and (3) with $\alpha=0.84$ and subtracted the fitted value from the experimental data to examine the systematic deviations. Figures 10(a) and 10(b) show the deviations for Eqs. (3) and (2), respectively. Even though the statistical deviations are comparable to the instrument resolution, the systematic deviations are significantly greater for the power law shown in Fig. 10(b). Since the exponent y of the general form shows little dependence on T and H , we fix it to a typical value of 1.15 and fit data for $H=5$ T at $T=8, 10, 12$, and 15 K, shown in Fig. 11 by curves (a)–(d), respectively. In Eqs. (2) and (3), the excess magnetization from the volume term, due to imbalance numbers of two sublattices in each domain, is not included since it is expected to be very small in comparison to the time-dependent term.^{18,15} We have also found from fitting data with a computer that including a small volume term in Eq. (3) yields very little change of χ^2 and can be neglected. On the other hand, Eq. (2) yields better fits with a significantly large *negative* value of B . Since $B < 0$ is unphysical, we attribute this result to the systematic deviations of the data from Eq. (2).

Often in the literature, equations like Eq. (3) appear with the time expressed with no clear normalization. The normalization is unimportant if t is large enough, i.e., $t \rightarrow \infty$, but this limit is not particularly helpful for laboratory experiments. In our fitting, we usually normalized time arbitrarily to 1 sec, i.e., $t'=1$ sec, in the absence of any theoretical prediction. The ambiguity in normalization affects the parameters obtained in the fit, particularly the exponent value. There is, however, one clear feature which can be established independently of the normaliza-

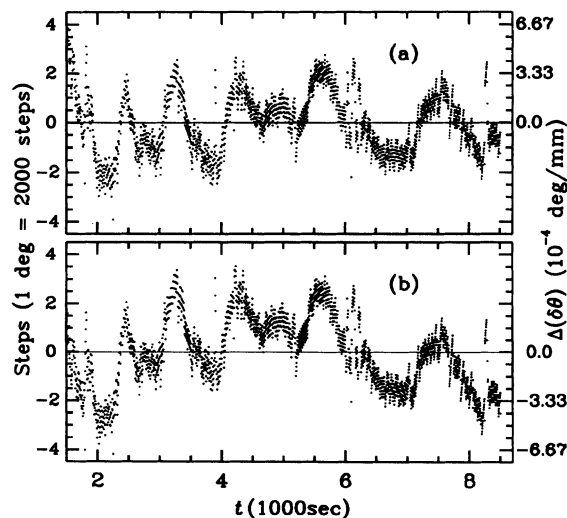


FIG. 10. The deviation of the fits to Eqs. (2) and (3) from the data vs t . The data set used in this comparison is the same as that shown in Fig. 9. (a) shows the deviations of the fit to the general form in Eq. (3) from the data. (b) shows the deviations of the fit to the power law in Eq. (2) from the data. The systematic deviations are clearly smaller for the generalized form. This behavior is shared by all the data sets.

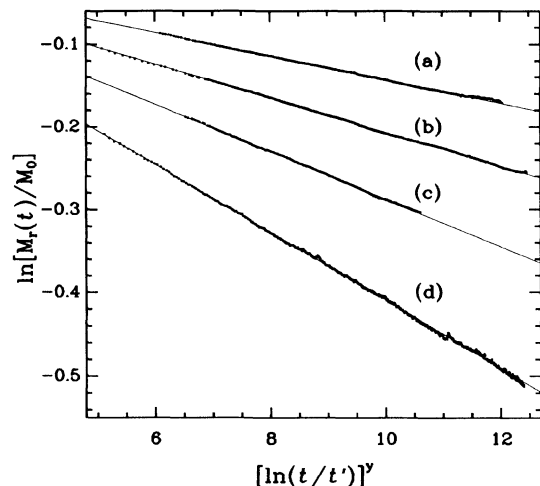


FIG. 11. $\ln[M_r(t)/M_0]$ vs $[\ln(t/t')]^y$ with $y=1.15$ for the data and the best fit to the general form, Eq. (3). The data are for $H=5$ T at different temperatures: (a) 8 K, (b) 10 K, (c) 12 K, and (d) 15 K. The straight lines are the fits to the data. For $T=12$ K, the whole range of data is not used because of instrumental instabilities which are not readily visible in Fig. 1, but make fitting difficult nevertheless. This figure shows that all of the data may be described by a common exponent.

tion. The three categories, i.e., $y > 1$ (faster relaxation than the power law), $y=1$ (the power law), and $y < 1$ (slower relaxation), are not interchanged by using different normalization values and the sign of the exponent is therefore well determined. The relaxation is faster than that indicated in the power law [Eq. (2)]. We note that an extraordinarily large range of time would be required in the measurements to determine the proper normalization from the fits to the data.

Even though no theoretical support is found in the literature to describe the behavior observed in these experiments with Eq. (3), equations of the same general form are used to describe other magnetic systems with quenched randomness. The relaxation in the Griffiths phase²⁹ has the form of Eq. (3) with $y=d/(d-1) > 1$. However, the Griffiths phase temperature range for the diluted antiferromagnet is between T_N of the diluted system and T_N of the corresponding pure one. The temperature range of our study is much below $T_c(H) < T_N$ of the diluted system. Hence, the theory is not directly applicable to our experiments. Using the droplet model, Huse and Fisher³⁰ have proposed the function which has the same form of Eq. (2) for the long-time dynamics of the autocorrelation function in the equilibrium state. They proposed the exponent values with $y=1$ for the random-exchange Ising model and $y=(d-2)/(d-1) < 1$ for the random-field Ising model. In this droplet, model fluctuations in the long-range order are thermally activated in equilibrium when T is less than T_c . The system which we study here involves relaxation via nonequilibrium dynamics. The field-cooled metastable domains are not induced by thermal fluctuations. Therefore, this theory is also not directly applicable to our experiment.

It is interesting to note how slowly the excess magnetization actually decays in this system. We can define a characteristic time τ' as the time when the excess magnetization decays to a value $M_0 e^{-1}$, i.e., $\ln(\tau'/t') = A^{-1/y}$. Using the normalization $t'=1$ sec, the value $y=1.15$, and the range $0.04 > A > 0.015$ found in these experiments, the characteristic time ranges from 0.5 to 10^9 yr (note that this result is independent of the normalization chosen). This extremely slow relaxation, due to the magnetic vacancies and large anisotropy, apparently occurs only for small enough temperature ($T \ll T_N/2$). For $T > 0.5 T_N$, the domain growth is probably thermally activated. Similar effects attributed to domain growth at high temperature were also seen in the experiment with $\text{Fe}_{0.7}\text{Mg}_{0.3}\text{Cl}_2$ (Ref. 20) and in computer simulation.²³

Finally, we note that magnetization studies³¹ in $\text{Rb}_2\text{Co}_{0.60}\text{Mg}_{0.40}\text{F}_4$ have shown qualitatively similar effects, i.e., extremely slow relaxation after removing the field. Since this system is very close to the percolation threshold, we cannot directly compare the behavior of the two systems.

V. CONCLUSIONS

We have measured the Faraday rotation of the excess magnetization resulting from the metastable domain structure induced by FC in the diluted Ising antiferromagnet $\text{Fe}_{0.47}\text{Zn}_{0.53}\text{F}_2$. We have examined several functions in an attempt to fit data for the decay of the remanent magnetization. First, the NV function Eq. (1) does not adequately describe the data obtained in our experimental region of temperature and field. It is an open question whether the NV predictions will hold at temperatures $T < 5$ K, below the present range. The power law in Eq. (2), suggested by earlier Monte Carlo studies, is a better function for fitting our data. This seems to hint at some inadequacy of the NV treatment of the relaxation of fractal domains. Even though the relaxation of fractals very probably should result in a self-similar time dependence, i.e., a power law, the generalized form with $y > 1$, Eq. (3), shows even better fits to the data. It has one additional feature in that the exponent y is largely T and H independent. We also note that this general form Eq. (3) with $y > 1$ describes very well the Monte Carlo results for the bcc diluted Ising antiferromagnet model.²⁷ Although this form has been used in various theories for the dynamics of magnets with quenched disorder, the theories are not directly applicable to our experiments. Clearly, more theoretical work is definitely called for in order to justify either the conventional or the generalized power-law behavior.

Note added. It has been pointed out by T. Nattermann (private communication) that the original NV theory can be modified to yield a power-law behavior in the decay of the remanent magnetization. It is suggested that the power-law dependence of ΔE on the length scale L (Ref. 18) can be replaced by a logarithmic one. This would transform the logarithmic time dependence of the remanent magnetization given in the original NV theory into a power-law dependence.

ACKNOWLEDGMENTS

We would like to thank M. Duncan for construction of part of the apparatus and Vince Jaccarino for the high-

quality crystal. The work at UCSC was supported in part by DOE Grant No. DE-FG03-87ER45324. The work at Universität Duisburg was supported by the Deutsche Forschungsgemeinschaft through Sonderforschungsbereich 166.

-
- ¹J. Villain, *Phys. Rev. Lett.* **52**, 1543 (1984).
²R. Bruinsma and G. Aeppli, *Phys. Rev. Lett.* **52**, 1547 (1984).
³G. Grinstein and J. F. Fernandez, *Phys. Rev. B* **29**, 6389 (1984).
⁴V. Jaccarino and A. R. King, *Physica A* **163**, 291 (1990).
⁵D. P. Belanger, *Phase Transitions* **11**, 53 (1988).
⁶T. Nattermann and J. Villain, *Phase Transitions* **11**, 5 (1988).
⁷D. P. Belanger, B. Farago, V. Jaccarino, A. R. King, C. Lartigue, and F. Mezei, *J. Phys. (Paris) Colloq.* **49**, C8-1229 (1988).
⁸S. Fishman and A. Aharony, *J. Phys. C* **12**, L729 (1979).
⁹D. P. Belanger, A. R. King, and V. Jaccarino, *Phys. Rev. B* **31**, 4538 (1985).
¹⁰H. Yoshizawa, R. A. Cowley, G. Shirane, and R. Birgeneau, *Phys. Rev. B* **31**, 4548 (1985).
¹¹A. R. King, J. A. Mydosh, and V. Jaccarino, *Phys. Rev. Lett.* **56**, 2525 (1986).
¹²A. E. Nash, A. R. King, and V. Jaccarino, *Phys. Rev. B* **43**, 1272 (1991).
¹³D. P. Belanger, A. R. King, V. Jaccarino, and J. L. Cardy, *Phys. Rev. B* **28**, 2522 (1983).
¹⁴K. E. Dow and D. P. Belanger, *Phys. Rev. B* **39**, 4418 (1989).
¹⁵P. Pollak, W. Kleemann, and D. P. Belanger, *Phys. Rev. B* **38**, 4773 (1988).
¹⁶M. Lederman, J. Selinger, R. Bruinsma, J. M. Hammann, and R. Orbach (unpublished).
¹⁷T. Nattermann, *J. Phys. A* **21**, L635 (1988).
¹⁸T. Nattermann and I. Vilfan, *Phys. Rev. Lett.* **64**, 223 (1988).
¹⁹W. Kleemann, A. R. King, and V. Jaccarino, *Phys. Rev. B* **34**, 479 (1986).
²⁰U. A. Leitão, W. Kleemann, and I. B. Ferreira, *Phys. Rev. B* **38**, 4765 (1988).
²¹U. A. Leitão, W. Kleemann, and I. B. Ferreira, *J. Phys. (Paris) Colloq.* **49**, C8-1217 (1988).
²²U. Nowak and K. D. Usadel, *Phys. Rev. B* **39**, 2516 (1989).
²³U. Nowak and K. D. Usadel, *Phys. Rev. B* **43**, 851 (1991); *Physica B* **165**, 211 (1990).
²⁴F. C. Montenegro, A. R. King, V. Jaccarino, S-J. Han, and D. P. Belanger, *Phys. Rev. B* **44**, 2155 (1991).
²⁵J. Cardy, *Phys. Rev. B* **29**, 505 (1984).
²⁶M. T. Hutchings, B. D. Rainford, and H. J. Guggenheim, *J. Phys. C* **3**, 307 (1970).
²⁷S-J. Han and D. P. Belanger (unpublished).
²⁸U. Nowak and K. D. Usadel, *Phys. Rev. B* **44**, 7426 (1991).
²⁹M. Randeria, J. P. Sethna, and R. G. Palmer, *Phys. Rev. Lett.* **54**, 1321 (1985).
³⁰D. A. Huse and D. S. Fisher, *Phys. Rev. B* **39**, 6841 (1987).
³¹H. Ikeda, Y. Endoh, and S. Itoh, *Phys. Rev. Lett.* **64**, 1266 (1990).